DESIGN AND VALIDATION OF A SURFACE PROFILING APPARATUS FOR AGRICULTURAL TERRAIN ROUGHNESS MEASUREMENTS

/

农田地面不平度测试装置的设计与验证

Jianguo Yan, Chunguang Wang*), Shengshi Xie, Lijuan Wang [1]
College of Mechanical and Electrical Engineering, Inner Mongolia Agricultural University, Hohhot 010018, China
Tel: +86 13624713647; E-mail: nmndwcg@126.com
DOI: 10.35633/INMATEH-59-19

Keywords: *agricultural terrain profiles, field surface roughness, profiling apparatus, profiling validation*

ABSTRACT

How to accurately and efficiently measure the profiles of the terrain on which agricultural machines operate has been an ongoing research topic. In this study, a surface profiling apparatus (profiler) was developed to measure agricultural terrain profiles along parallel tracks. The profiler is mainly composed of sensor frames, an RTK-GNSS system (Real Time Kinematics-Global Navigation Satellite Systems), laser sensors, an Inertial Measurement Unit (IMU) sensor and a data acquisition system. Along with a full description of how the terrain profiles were produced, a methodology to compensate for the tractor motion was included in the sensor data analysis. In field profiling validation, two trapezoidal bumps with known dimensions were used to assess the ability of the terrain profiler to reproduce the vertical profiles of the bumps, resulting in root mean square error (RMSE) of 3.6-4.7 mm and 4.5-5.1 mm with profiling speeds of 1.02 and 2.56 km/h, respectively. In addition, a validation test was also conducted on an asphalt road by profiling a flat road with the measuring wheels of the profiler rolling on the flat section but with the tractor wheels driving over a trapezoidal bump to excite the tractor pitch and roll motion. The measured profiles then also exhibited a flat road, which showed the ability of the profiler to remove the tractor motion from the profiling measurements.

摘要

如何准确、高效地测量农业机械所接触的农田地面不平度一直是研究者们关注的问题。本文设计了一种可并排测量农田地面不平度的装置，主要由传感器架、RTK-GNSS 系统、激光传感器、IMU 传感器和数据采集系统等部分组成。在数据分析中，除了对地面不平度的生成进行了完整描述外，提出了一种补偿拖拉机运动的方法。农田试验中，利用两个尺寸已知的梯形凸台检验不平度测试装置再现凸台垂直剖面的性能，当测试速度分别为 1.02 和 2.56 km/h 时，不平度均方根误差范围分别为 3.6-4.7 mm 和 4.5-5.1 mm。另外，在沥青路面上也开展了验证试验，方法是对平坦沥青路面进行不平度测试，使不平度测试装置的地轮在平坦路面上滚动，而拖拉机车轮经过一个梯形凸台，以激励其产生俯仰和侧倾运动。测量的不平度结果依然反映的是一条平坦的路面，证明了不平度测试装置从测量值中去除拖拉机运动成分的有效性。

INTRODUCTION

Agricultural tractors and implements usually operate on very rough terrain and are vibrated by the displacement of the field profiles acting on each wheel during operation in an agricultural field. The vibration restricts the work efficiency and operation quality of the agricultural machinery (*Ren Wentao et al., 2009; Zhao Manquan et al., 2012*), which also causes parts of the agricultural machines to bear a great dynamic load (*Clijmans L. et al., 1998*), and seriously endangers the health of the driver (*Liang X. C. et al., 2018; Niu P. et al., 2017*). To study the dynamic response characteristics of agricultural machinery caused by terrain roughness, terrain profiles should be investigated. This arises a problem that is how to accurately and efficiently measure the agricultural terrain profiles that agricultural machines operate on.

Profiling instruments have become the standard tools for investigating road roughness.

[1] *Jianguo Yan, As. Ph.D. Stud. Eng.; Chunguang Wang, Prof. Ph.D. Eng.; Shengshi Xie, Lect. Ph.D. Eng.; Lijuan Wang, Lect. M.S. Eng.*

However, these instruments are not suitable for measuring agriculture-related profiles due to the large unevenness of fields and the impact of weeds or crop stubble on the profiling results. There are mainly two types of profiling instruments developed for achieving the agricultural terrain roughness measurement: static profiling apparatus and dynamic profiling apparatus (*Sayers M. W. et al., 1998*). The rod and level are familiar static measuring tools. This method is referred to as “static” because the instruments are stationary when the profile elevation measures are taken. A micro laser relief meter, a static profiler, was designed to measure soil profiles with the maximum test distance of 1 meter at a time (*Lu Z. X. et al., 2005*). Obviously, it is very time consuming and resource intensive to measure hundreds of meters of terrain profiles.

Dynamic profiling instruments are preferred and make highly efficient profiling possible for investigating the roughness of agricultural terrain. The first attempt to build a high-speed profiler was made by Spangler (*Spangler E.B. et al., 1966*). Accelerometers were commonly used to characterize road roughness based on vehicle responses such as spindle acceleration and load (*González A. et al., 2008*). These inertial profilers relying on accelerometers to measure the vertical position suffer at low host vehicle speeds due to their limited accelerometer bandwidth (*Walker R.S. et al., 2006*). Because modern measurements require high resolution and large vertical dynamic measuring ranges, terrain measurement technology has progressed from inertial profilers to optical techniques such as laser distance-measuring instruments for field profile measurement (*Paraforos D.S. et al., 2016*). Vision acquisition has also been incorporated for characterizing the surface roughness of different terrains (*Howard A. et al., 2001*).

With the aim of measuring agricultural-related profiles, a profiling apparatus was developed with the following capabilities: producing high profiling efficiency, avoiding the impact of weeds or crop stubble on the profiling results and effectively removing the tractor motion from the profiling measurements.

MATERIALS AND METHODS

Instrumentation

As shown in Fig. 1, the profiler was mounted on the front counterweight of a tractor, which makes it easy to further analyse the coupling vibration between the tractor and the field ground because the profiles measured are the ones that will vibrate the tractor when the tractor wheels roll on the profile path. The profiler comprises two sensor frames mounted on the front counterweight of a tractor, two laser sensors (Banner LT3NU W/30, USA) for measuring the distance from the sensor frame *1* to a metal plate mounted on each wheel, a RTK-GNSS system (Trimble AgGPS 542 RTK-GNSS, USA) for providing geo-reference of the measured data, an IMU (LMRK 20 AHRS, USA) for providing real-time tilt (roll-pitch-yaw) information of the tractor, and a data acquisition system for receiving and saving all sensor data in parallel.

Fig. 1 - Profiling apparatus mounted on the front counterweight of a tractor

The schematic diagram of the sensor frame 1 is illustrated in Fig. 2.

The frame was mounted on the front counterweight of a tractor via two connecting rods under a connecting seat and was fixed by fastening nuts. The sensor frame was supported by two road-following wheels with widths of 125 mm and diameters of 200 mm. A suitable wheel material, such as nylon, was chosen to maintain a low wheel mass and reduce the vibration from the wheels to the frame. To prevent soil compaction while maintaining contact with the profiled surface, stainless steel square tubes with transverse dimensions of 40*40*2.5 mm were utilized to minimize the mass of the sensor frame. The static load of each wheel on the ground surface was measured to be 32 N. Therefore, it can be approximated that the wheels do not change the elevations of the ground surface and the field surface roughness can be effectively reflected by the up-and-down motions of the wheels. Additionally, springs, in which the preload can be adjusted by nuts, were added to push the wheels towards the surface ground.

Referring to Fig. 2, two parallelogram linkages in the profiler, which are connected to the two wheels, ensure that the metal plates move up and down and the motion of each plate is always “parallel” to the ground. Each parallelogram linkage comprises an upper hinged plate, a lower hinged plate, a wheel guided rod, a sleeve guided rod and two adjusting sleeves. The parallelogram linkages and supported wheels were driven by two drag beams that were rotatably mounted to connecting seat by a pin shaft.

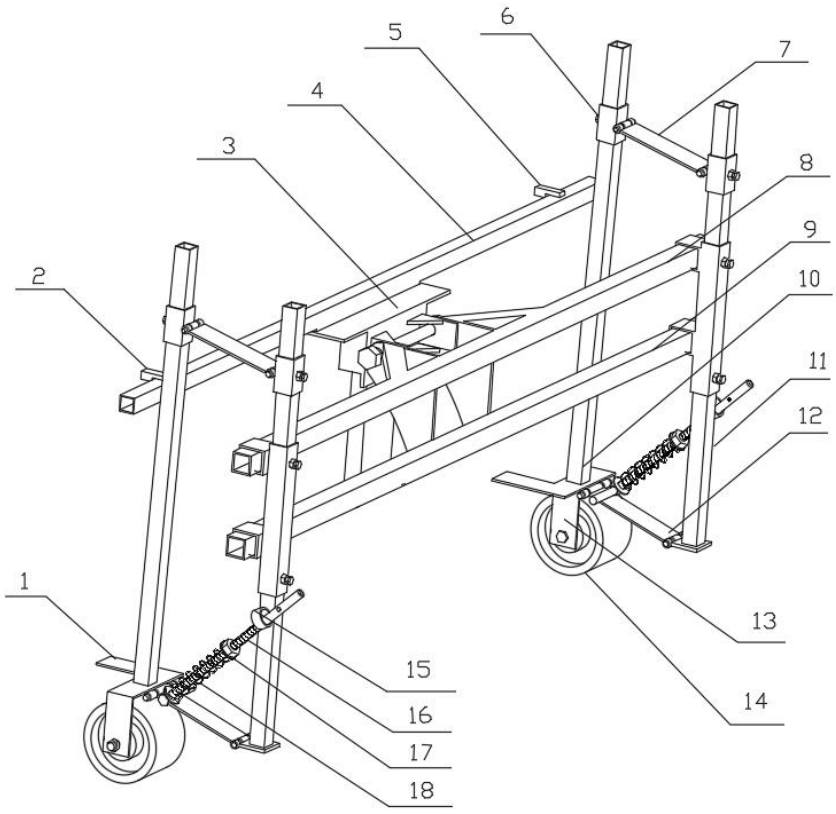

Fig. 2 - Schematic diagram of the sensor frame 1 of the profiler

1- Metal plate; 2-Laser sensor 1; 3-Connecting seat; 4-Sensor beam; 5-Laser sensor 2; 6-Adjusting sleeve; 7-Upper hinged plate; 8-Drag beam 1; 9-Drag beam 2; 10-Wheel guide rod; 11-Sleeve guide rod; 12-Lower hinged plate; 13-Wheel axle; 14-Road-following wheel; 15-Inclined hole; 16-Threaded rod; 17-Nut; 18-Spring

The IMU and GNSS antenna were attached on sensor frame 2, which was mounted on the front counterweight of the tractor to ensure that the IMU and GNSS antenna align on the longitudinal centre plane of the tractor.

Two laser sensors with measuring distances of 0.3-5 m were attached on a sensor beam and symmetrical to the longitudinal centre plane of the tractor. To avoid the impact of weeds or crop stubble on the field surface profiling, the relative vertical distances from the sensor beam to the metal plates mounted on each wheel axle were measured with two laser sensors. The positions of the road-following wheels and the laser sensors were adjustable so that surface profiles of the parallel tracks with different widths could be measured. The road-following wheels could also be adjusted to 30 cm high from the ground surface after the profile measurement, which did not affect the normal operation of the tractor.

Data acquisition software was developed in LabVIEW for acquiring and recording all sensor data in parallel, as shown in Fig. 3. A computer and a virtual instrument were necessary to acquire the signals and readings obtained from the measuring sensors carried on the profiler and its driving vehicle. This data acquisition system could also be extended to synchronously measure the field terrain surface profiles and dynamic responses of the tractor-caused by the surface roughness, which provides a possibility for further study regarding the coupling vibration characteristics of terrain roughness and vehicle dynamics.

Fig. 3 – Software interface of profiling data acquisition system

Profiling validation test

The location of the profiling validation test was situated at 40.21°N latitude and 111.34°E longitude in Hohhot, China, and the test was completed on October 5, 2019.

The validation test took place in a harvested corn field to provide close to real-world operating conditions, as shown in Fig. 4.

Fig. 4 - Field profiling validation test

Two trapezoidal bumps with known dimensions were used to verify the ability of the terrain profiler to reproduce the vertical profiles of the bumps. In addition, a validation test was also conducted on an asphalt road by profiling a flat road with the road-following wheels of the profiler rolling on the flat section but with the tractor wheels on one side driving over a bump to excite tractor pitch and roll motion, as shown in Fig. 5.

Fig. 5 - Asphalt road profiling validation test

The laser and positioning systems were also evaluated concurrently with digital signal processing techniques to compensate for vehicle body motion. Whether the measured results always reflect a flat road could indicate the ability of the profiler to remove the tractor motion from the laser measurements. During all validation tests, the tractor was maintained at two constant forward speeds of 1.02 and 2.56 km/h. The tire pressure of the tractor was 230 kPa in the front and 200 kPa in the rear.

The two trapezoidal bumps were made of wood, and their dimensions are shown in Fig. 6. Such bumps are commonly used for road profile validation (*Becker C.M. et al, 2014; Smith H. et al, 2010*). A 0.7-metre bump was used on the left track, while a 0.9-metre bump was used on the right track with the road-following wheels of the profiler rolling over the bumps in the field validation test. A 0.7-metre bump was used on the left track to excite the tractor pitch and roll motion in the asphalt road validation test.

The difference between the measured profile and the actual profile of the bump can be expressed quantitatively as the root mean square error (*RMSE*) using equation (1) below:

$$RMSE = \sqrt{\frac{\sum_{i=1}^{n}(Z_{mi} - Z_{ai})^2}{n}} \quad (1)$$

where: Z_{mi} is the measured profile of the bump for time instance i;

Z_{ai} is the actual profile of the bump for time instance i;

n is the number of measured points for the bump profile.

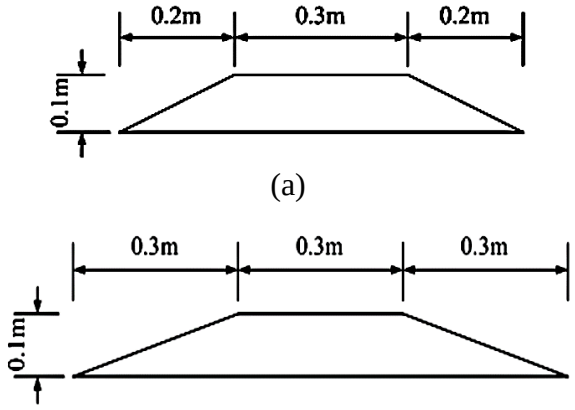

Fig. 6 - Trapezoidal bump dimensions
(a) 0.7-meter bump (b) 0.9-meter bump

THEORY

The tractor as a carrying vehicle influences the built sensor frame. Especially in agricultural terrains, potholes and bumps are common and even sudden changes in the terrain inclination. In this way, the motion of the tractor is combined with the motion of the terrain in the laser measurements. Thus, the laser movement caused by the roll and pitch motion of the tractor needs to be deducted from the profiling measurements. In this study, along with a full description of how the terrain profiles were being produced, a methodology to compensate for the tractor motion was included in the sensor data analysis.

Coordinate transformation

An RTK-GNSS was used to provide absolute geo-referenced coordinates of the measured data. Using the real-time dynamic tilt information (roll-pitch-yaw) provided by the IMU, the motion of the lasers on the sensor frame could be calculated through coordinate transformation.

The position data obtained directly through RTK-GNSS receiver are the latitude φ, longitude λ and altitude h, which are expressed in WGS-84 (World Geodetic System-1984) coordinates. The output data from the IMU, such as the angles of roll ψ, pitch θ, and yaw ϕ, are based on vehicle body coordinates. To integrate the data acquired from the RTK-GNSS and the IMU, it is necessary to convert the GNSS data coordinates into vehicle body coordinates. This procedure requires that the RTK-GNSS data be converted to the Earth-Centered Earth-Fixed (ECEF) coordinates, then to the NED coordinates, and finally to the vehicle body coordinates.

If $P_E = \left[X_E, Y_E, Z_E\right]^T$ is the position in ECEF coordinates, the conversion from the WGS-84 coordinates to the ECEF coordinates can be performed using the following equations (*Farrell J. et al, 1999*):

$$X_{\mathrm{E}} = (N(\varphi) + h)\cos(\varphi)\cos(\lambda) \tag{2}$$

$$Y_{\mathrm{E}} = (N(\varphi) + h)\cos(\varphi)\sin(\lambda) \tag{3}$$

$$Z_{\mathrm{E}} = \left[N(\varphi)(1-e^2) + h\right]\sin(\varphi) \tag{4}$$

where:

$e = 0.0818$ is the first numerical eccentricity of the earth ellipsoid;

N is the distance from earth's surface to the Z-axis along the ellipsoid normal given by:

$$N = \frac{a}{\sqrt{1 - e^2 \sin^2 \varphi}} \tag{5}$$

where:

$a = 6378137$ m is the semi-major axis length of the earth.

If $P_N = \left[X_N, Y_N, Z_N\right]^T$ is the position in the local NED coordinates, the conversion from the ECEF coordinates to the NED coordinates is

$$P_{\mathrm{N}} = R_{\mathrm{N/E}} \cdot P_{\mathrm{E}} \tag{6}$$

where:

$R_{N/E}$ is the transformation matrix from the ECEF coordinates to the NED coordinates.

$$R_{\mathrm{N/E}} = \begin{bmatrix} -\sin\varphi\cos\lambda & -\sin\varphi\sin\lambda & \cos\varphi \\ -\sin\lambda & \cos\lambda & 0 \\ -\cos\varphi\cos\lambda & -\cos\varphi\sin\lambda & -\sin\varphi \end{bmatrix} \tag{7}$$

If $P_B = \left[X_B, Y_B, Z_B\right]^T$ is the position in the vehicle body coordinates, the conversion from the NED coordinates to the vehicle body coordinates is

$$P_{\mathrm{B}} = R_{\mathrm{B/N}} \cdot P_{\mathrm{N}} \tag{8}$$

where:

$R_{B/N}$ is the transformation matrix from the NED coordinates to the vehicle body coordinates (*Farrell J. et al., 1999*):

$$R_{B/N} = \begin{bmatrix} \cos\theta\cos\psi & \cos\theta\sin\psi & -\sin\theta \\ \sin\phi\sin\theta\cos\psi - \cos\phi\sin\psi & \sin\phi\sin\theta\sin\psi + \cos\phi\cos\psi & \sin\phi\cos\theta \\ \cos\phi\sin\theta\cos\psi + \sin\phi\sin\psi & \cos\phi\sin\theta\sin\psi - \sin\phi\cos\psi & \cos\phi\cos\theta \end{bmatrix} \quad (9)$$

Measured profile calculation

The parallel profiles were calculated using the known dimensions of the sensor frame and the measured distances provided by the two laser sensors. With compensation for the tractor motion, the motion of the lasers on the sensor frame was deducted from the profiling measurements.

Fig. 7 - Coordinates of x (Roll), y (Pitch) and Z (Yaw) on the IMU

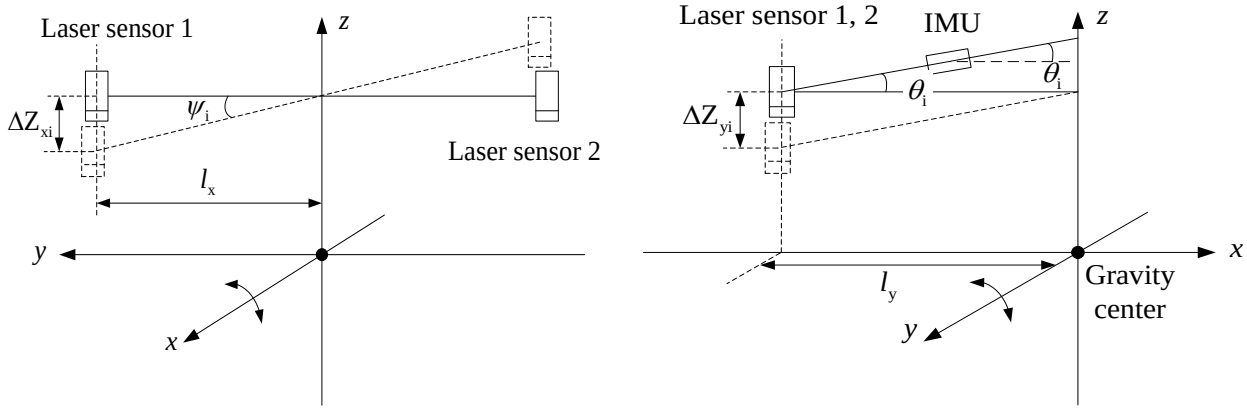

a) b)

Fig. 8 - Vertical displacement change of the laser sensors caused by tractor motion

(a) Roll motion (b) Pitch motion

The coordinates of X (roll), Y (pitch) and Z (yaw) on the IMU are shown in Fig. 7. The attachment of the IMU could ensure that the X-axis of the IMU was on the longitudinal centre plane of the tractor. In relation to the tractor body, the positive directions of the axes are X - backward, Y - left and Z - upward. The roll-pitch-yaw angle values of the IMU comply with the right-hand rule. Fig. 8 shows the vertical displacement change in the laser sensors caused by the roll and pitch motion of the tractor.

With compensation for the tractor motion, the expression of the measured profile is as follows:

$$Z_m = -(Z_i - Z_0 \pm \Delta Z_{xi} + \Delta Z_{yi}) \quad (10)$$

where:

$Z_m (m=0,1,\ldots, N-1)$ are the measured surface roughness heights of each profile;

Z_i is the vertical distance the laser sensor measured for time instance i;

Z_0 is the vertical distance from laser sensor to the metal plate when the tractor is placed horizontally (Fig. 2).

$\Delta Z_{xi} = l_x \tan\psi_i$ is the vertical displacement change of the laser sensors caused by the roll motion of the tractor at the i th measuring point, seen as Fig. 8 (a). For laser sensor 1, the value is taken as $+\Delta Z_{xi}$, while for laser sensor 2, the value is taken as $-\Delta Z_{xi}$. The parameter l_x is the distance from a laser sensor to the longitudinal centre plane of the tractor, and ψ_i is the tractor roll angle for time instance i.

$\Delta Z_{yi} = l_y \tan\theta_i$ is the vertical displacement change of the laser sensors caused by the pitch motion of the tractor at the i th measuring point, as shown in Fig. 8 (b). The parameter l_y is the longitudinal distance from a laser sensor to the gravity centre of the tractor, and θ_i is the tractor pitch angle for time instance i.

Assume the $Z_m (m=0,1,\ldots, N-1)$ are measured at equally spaced intervals Δx, then the measured surface profile roughness $Z(l)$ which is the Z_m as a function of longitudinal distance $l=m\Delta x$ could be fixed.

RESULTS

Field profiling validation results

The profiles measured while traversing two trapezoidal bumps in the harvested corn field in one of the validation tests with a profiling speed of 1.02 km/h are presented in Fig. 9. The accuracy of the profiler could be evaluated by comparing the actual profile of the bump to the profile as measured by the laser. The error between these signals was evaluated using the *RMSE* calculated by the equation (1).

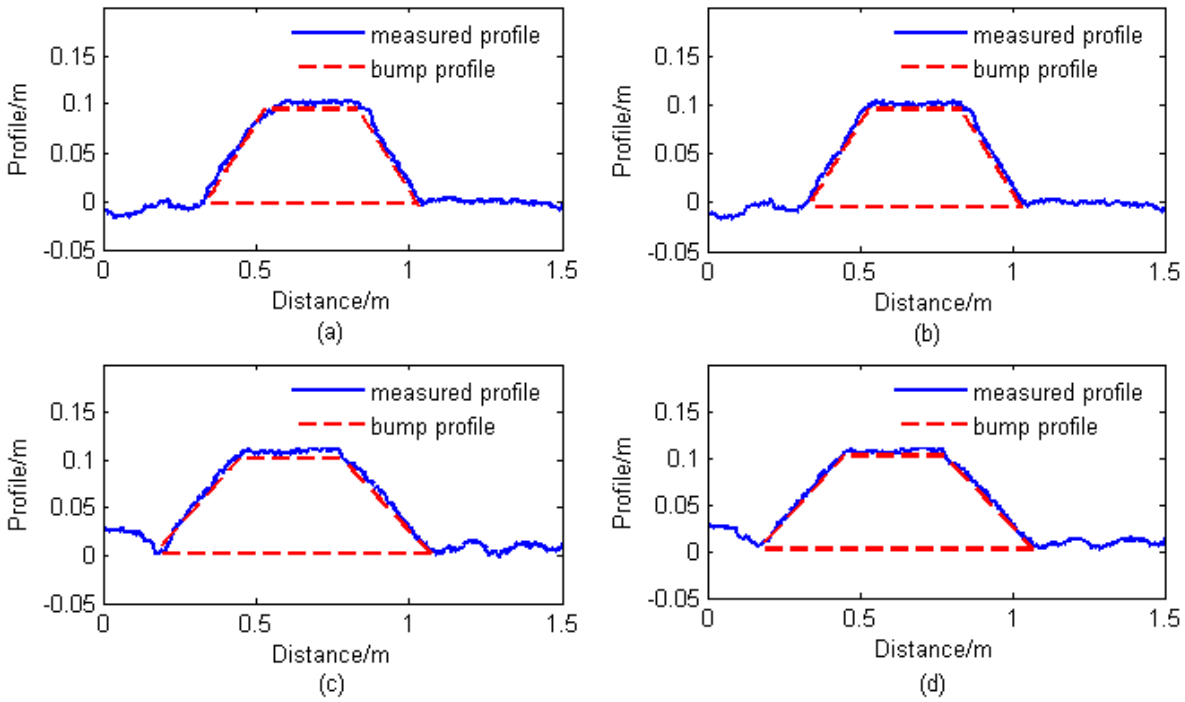

Fig. 9 - Measured profiles in one of the field profiling validation tests

(a) Measured profile of a 0.7-metre bump; (b) measured profile of a 0.7-metre bump with compensation for the tractor motion; (c) measured profile of a 0.9-metre bump; and (d) measured profile of a 0.9-metre bump with compensation for the tractor motion

It can also be seen from Fig. 9 that the measured profiles could reflect the elevations of the trapezoidal bumps. The overall agreement between the measured profiles and the actual profiles of the bumps was improved by compensating for the tractor motion. In Fig. 9, using equation (1), the *RMSE* values were calculated to be 5.8 mm and 5.2 mm for the left and right tracks, respectively, while they were reduced to 4.3 mm and 3.9 mm with compensation for the tractor motion.

The *RMSE* values in the field profiling validation tests were calculated and summarized in Table 1.

Table 1

Field profiling validation results

Test code	Left track bump profile		Right track bump profile	
	***RMSE* value with no compensation [mm]**	***RMSE* value with compensation [mm]**	***RMSE* value with no compensation [mm]**	***RMSE* value with compensation [mm]**
A1	5.8	4.3	5.2	3.9
A2	5.6	4.7	5.4	4.6
A3	5.1	3.6	4.9	3.8
B1	6.0	5.1	6.2	4.9
B2	6.1	4.8	5.8	4.7
B3	6.4	4.9	5.7	4.5

The test code letters A and B indicate validation tests with profiling speeds of 1.02 and 2.56 km/h, respectively. Different numbers (1, 2, 3) indicate three repeated treatments of each test.

In Table 1, the *RMSE* values ranged from 4.9 mm to 5.8 mm and from 5.7 mm to 6.4 mm, when the profiling speed was maintained at 1.02 km/h and 2.56 km/h, respectively. With compensation for the tractor motion, the *RMSE* values reduced to range from 3.6 mm to 4.7 mm and from 4.4 mm to 5.1 mm for profiling speeds of 1.02 km/h and 2.56 km/h, respectively.

According to Table 1, the comparison of the measured profile values is shown in Fig. 10.

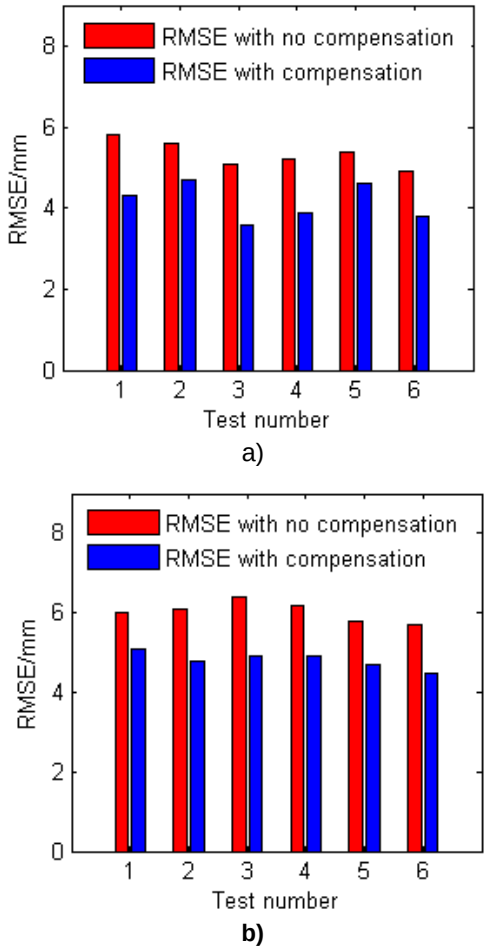

Fig. 10 - *RMSE* values of the field profiling validation results
(a) Profiling speed of 1.02 km/h; (b) Profiling speed of 2.56 km/h

As shown in Fig. 10, the RMSE values of the field profiling validation results decreased noticeably with compensation for the tractor motion.

Asphalt road profiling validation results

The profiles measured in one asphalt road validation test with a profiling speed of 1.02 km/h are presented in Fig. 11.

Fig. 11 (a) and (c) show that the measured profiles were significantly affected by the tractor body roll and pitch motion (4-8 m section) when the front and rear wheels on one side of the tractor passed through the bump. The profiling results calculated by equation (10) are shown in Fig. 11 (b) and (d). With compensation for the tractor motion, the measured profiles basically reflected a flat road, which could indicate the ability of the profiler to remove the tractor motion from the laser measurements.

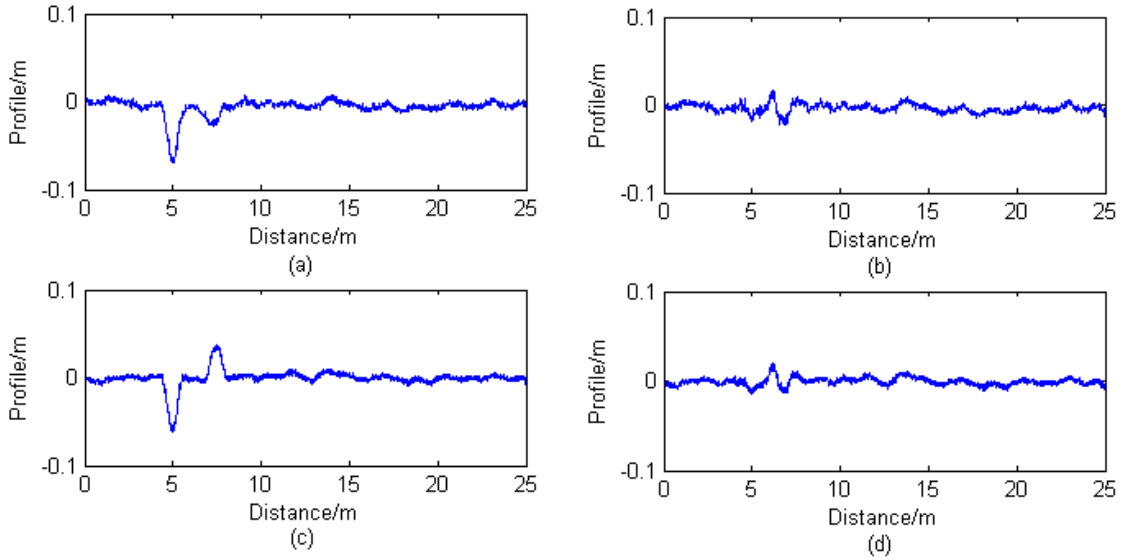

Fig. 11 - Measured profiles in one of the asphalt road validation tests

(a) Measured profile of the left track; (b) measured profile of the left track with compensation for the tractor motion; (c) measured profile of the right track; and (d) measured profile of the right track with compensation for the tractor motion

In Table 2, the $RMS_{4\text{-}8}$ values ranged from 24.3 mm to 28.1 mm and from 27.7 mm to 29.8 mm when the profiling speed was maintained at 1.02 km/h and 2.56 km/h, respectively. With compensation for the tractor motion, the $RMS_{4\text{-}8}$ values reduced to a range from 5.7 mm to 6.1 mm and from 6.1 mm to 6.8 mm for profiling speeds of 1.02 km/h and 2.56 km/h, respectively. The *RMS* values of the measured profiles on the whole test section of a flat asphalt road ranged from 5.5 mm to 5.8 mm and from 5.5 mm to 5.9 mm for profiling speeds of 1.02 km/h and 2.56 km/h, respectively.

The *RMS* values in the asphalt road profiling validation were calculated and summarized in Table 2.

Table 2

Asphalt road profiling validation results

Test code	Left track profile			Right track profile		
	$RMS_{4\text{-}8}$ value with no compensation [mm]	$RMS_{4\text{-}8}$ value with compensation [mm]	*RMS* value with compensation [mm]	$RMS_{4\text{-}8}$ value with no compensation [mm]	$RMS_{4\text{-}8}$ value with compensation [mm]	*RMS* value with compensation [mm]
A1	27.7	5.9	5.7	24.3	5.7	5.6
A2	28.1	5.8	5.5	24.6	5.9	5.7
A3	27.4	6.1	5.6	25.2	6.0	5.8
B1	29.5	6.6	5.8	27.7	6.6	5.9
B2	29.3	6.8	5.6	28.5	6.1	5.5
B3	29.8	6.4	5.6	29.1	6.2	5.8

The test code letters A and B indicate validation tests with profiling speeds of 1.02 and 2.56 km/h, respectively. Different numbers (1, 2, 3) indicate three repeated treatments of each test. $RMS_{4\text{-}8}$ represents the root mean square value of the measured profile on 4-8 m test sections, on which the tractor wheels on one side passed through a bump to excite pitch and roll motion. RMS represents the root mean square value of the measured profile on the whole test section of a flat asphalt road.

According to Table 2, the comparison of the measured profile values is shown in Fig. 12.

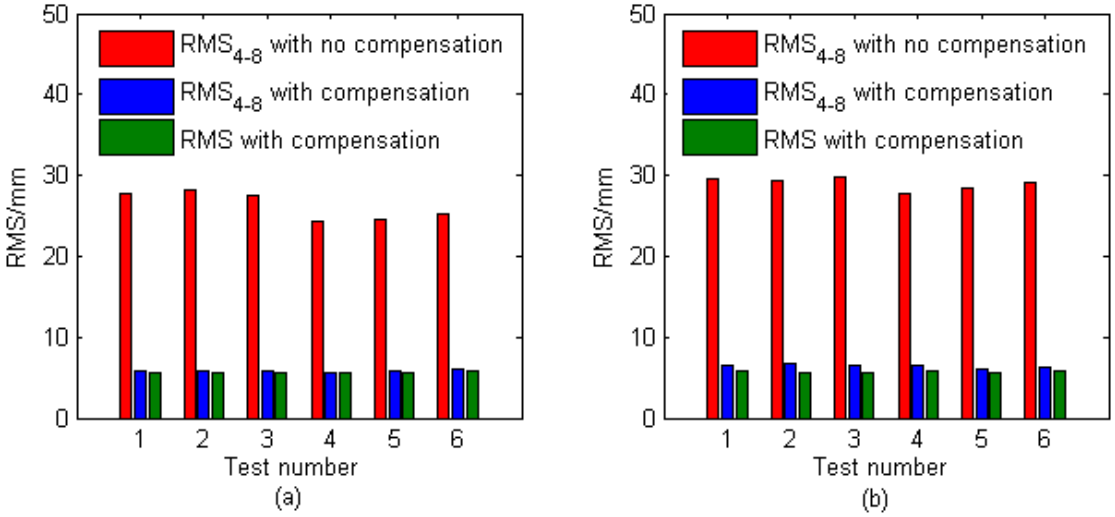

Fig. 12 - *RMS* values of the asphalt road profiling validation results

(a) Profiling speed of 1.02 km/h and (b) profiling speed of 2.56 km / h

From Fig. 12, comparing with no compensation for the tractor motion, the RMS_{4-8} values with compensation for the tractor motion were significantly reduced, and they were close to the *RMS* values of the measured profiles on the whole test section of a flat asphalt road.

These results indicate that the laser movement caused by the roll and pitch motion of the tractor can be effectively deducted from the profiling measurements and that the accuracy of the profiler is reliable.

CONCLUSIONS

The surface profiling apparatus (profiler) was designed to measure agricultural terrain profiles along parallel tracks. A methodology of how the terrain profiles were calculated and how to remove the tractor motion from the laser measurements was presented in the data analysis. To assess the accuracy of the developed profiler, profiling validation tests were carried out in a harvested corn field and on an asphalt road. Based on the profiling validation results and the analyses presented above, the following conclusions can be drawn:

(1) Using the developed profiler and the presented methodology, the agricultural terrain profiles on which the tractor was moving could be measured. The overall accuracy of the profiler, expressed by the root mean square error (RMSE) value, was 3.6-4.7 mm and 4.5-5.1 mm with profiling speeds of 1.02 km/h and 2.56 km/h, respectively. Considering the large size of the agricultural machinery tires, the resulting accuracy is regarded as adequate. With compensation for the vehicle body motion, the laser movement induced by the tractor roll and pitch motion could be effectively subtracted from the profiling measurements.

(2) The accuracy of the developed profiler was improved as the profiling speed was decreased. Thus, if very rough terrain is profiled, the most accurate profile will be obtained by profiling the terrain as slowly as possible.

ACKNOWLEDGEMENT

Special thanks are due to the Research Program of Science and Technology at Universities of Inner Mongolia Autonomous Region (NJZY20046), the National Natural Science Foundation of China (31901409), and the Natural Science Foundation of Inner Mongolia Autonomous Region (2019BS05012) for supporting authors' research.

REFERENCES

[1] Becker C.M., Els P.S., (2014), Profiling of rough terrain, *International Journal of Vehicle Mechanics and Mobility*, Vol. 64, Issue 2-4, pp. 240-261;

[2] Clijmans L., Ramon H., Baerdemaeker J. D., (1998), Structural modification effects on the dynamic behavior of an agricultural tractor, *Transactions of the ASABE*, Vol.41, Issue 1, pp.5-10;

[3] Farrell J., Barth M., (1999), The global positioning system & inertial navigation. McGraw-Hill Publishers, New York/U.S.A.;
[4] González A., O'Brien E. J., Li Y. Y., Cashell K., (2008), The use of vehicle acceleration measurements to estimate road roughness, *International Journal of Vehicle Mechanics and Mobility*, Vol. 46, Issue 6, pp. 483-499;
[5] Howard A., Seraji H., (2001), Vision-based terrain characterization and traversability assessment, *Journal of Robotic Systems*, Vol. 18, Issue 10, pp. 577-587;
[6] Liang X. C., Chen J., Wang Z., (2018), Research on the vibration of mini tiller, *INMATEH Agriculture Engineering*, vol. 56, issue 3, pp. 17-24;
[7] Lu Z. X., Nan C., Perdok U. D., Hoogmoed W. B., (2005), Characterisation of soil profile roughness, *Biosystems Engineering*, Vol. 91, Issue 3, pp.369-377;
[8] Niu P., Yang M. J., Chen J., Yang L., Xie S. Y., Chen X. B., (2017), Structural optimization of a handheld tiller handrail by vibration modal analysis, *INMATEH Agriculture Engineering*, vol. 52, issue 2, pp. 91-98;
[9] Paraforos D. S., Griepentrog H. W., Vougioukas S. G., (2016), Country road and field surface profiles acquisition, modelling and synthetic realisation for evaluating fatigue life of agricultural machinery, *Journal of Terramechanics*, Vol. 63, Issue 2, pp. 1-12;
[10] Ren Wentao, Lu Xiaorong, Zhang Benhua, (2009), Dynamic response of taped type rice direct seeding machine for field surface roughness, Transactions of the Chinese Society for Agricultural Machinery, Vol. 40, Issue 8, pp. 58-61;
[11] Sayers M. W., Karamihas S. M., (1998), *The little book of profiling-basic information about measuring and interpreting road profiles*, 100 p., University of Michigan Publishers, Michigan/U.S.A.;
[12] Spangler E. B., Kelly W. J., (1966), GMR road profilometer - a method for measuring road profile, *Highway Research Board*, Vol. 121, Issue 3, pp.27-54;
[13] Smith H., Ferris J. B., (2010), Calibration surface design and validation for terrain measurement systems, *Journal of Testing and Evaluation*, Vol. 38, Issue 4, pp. 431-438;
[14] Walker R. S., Becker E., (2006), Collecting stop and go inertial profile measurements, *Pavement Management Systems*, Vol. 20, Issue 2, pp. 56-65;
[15] Zhao Manquan, Hu Yongwen, (2012), Measurement and analysis on vibration characteristics of pneumatic seed metering device of no-till seeder. *Transactions of the Chinese Society of Agricultural Engineering*, Vol. 28, Issue 2, pp.78-83.